

Nanoscale

Accepted Manuscript



This is an *Accepted Manuscript*, which has been through the Royal Society of Chemistry peer review process and has been accepted for publication.

Accepted Manuscripts are published online shortly after acceptance, before technical editing, formatting and proof reading. Using this free service, authors can make their results available to the community, in citable form, before we publish the edited article. We will replace this *Accepted Manuscript* with the edited and formatted *Advance Article* as soon as it is available.

You can find more information about *Accepted Manuscripts* in the [Information for Authors](#).

Please note that technical editing may introduce minor changes to the text and/or graphics, which may alter content. The journal's standard [Terms & Conditions](#) and the [Ethical guidelines](#) still apply. In no event shall the Royal Society of Chemistry be held responsible for any errors or omissions in this *Accepted Manuscript* or any consequences arising from the use of any information it contains.

Cite this: DOI: 10.1039/c0xx00000x

www.rsc.org/xxxxxx

ARTICLE TYPE

Writing Nanopatterns with Electrochemical Oxidation on Redox Responsive Organometallic Multilayers by AFM

Jing Song,^a Mark A. Hempenius,^b Hong Jing Chung^c and G. Julius Vancso^{b,*}*Received (in XXX, XXX) Xth XXXXXXXXX 20XX, Accepted Xth XXXXXXXXX 20XX*

DOI: 10.1039/b000000x

Nanoelectrochemical patterning of redox responsive organometallic polyferrocenylsilane (PFS) multilayers is demonstrated by electrochemical dip pen lithography (EDPN). Local electrochemical oxidation and Joule heating of PFS multilayers from the tip are considered as relevant mechanisms related to structure generation. The influence of applied bias potential, tip velocity, and multilayer thickness on the pattern height and width were investigated.

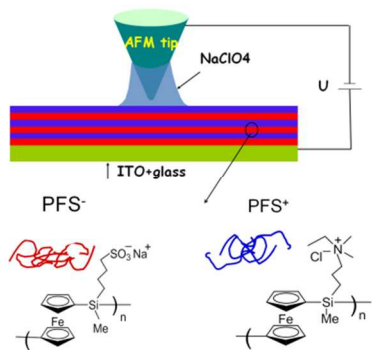
Fabrication of nanopatterns exposed at surfaces of polymer thin films is currently of great interest for developing organic electronic nanodevices and for sensor technologies.¹⁻³ Scanning probe microscopy (SPM) based lithographic techniques have proven to be extremely flexible patterning platforms with high spatial precision at the nanoscale, and without the necessity to use complex processing steps in comparison to other patterning techniques.^{4,5} Various force assisted lithography approaches such as physical probe nanolithography, dip pen nanolithography (DPN) and bias assisted lithography, including probe anodic oxidation, electrostatic nanolithography, and electrochemical DPN, have been developed to obtain controlled and well defined nanostructures with SPM.^{4, 6-8} For example, by adjusting the set point force of an AFM probe, well controlled nanopatterns have been written on an Au-Pd film evaporated on mica using the AFM indentation method.⁹ In electrostatic nanolithography, the “raised” patterns from a thin polymer film can be created by mass transport based on localized Joule heating by an applied electric field without any chemical crosslinking, substantial polymer degradation or ablation.^{7, 10} In thermal probe nanolithography, highly localized heat at the tip-sample contact area is used to transcribe patterns or images to a surface. For example, the heated tip can be used to evaporate solvent in the resist or decompose the polymer layer in thin films.^{11, 12}

For creating customized patterns in surface chemistry, DPN is a promising method which transfers and directs “ink molecules” from the “ink” coated AFM tip to a surface.⁸ This method has been successfully employed to create biomolecular nanoarrays and templates for the self-assembly of nanoparticles.^{13, 14} Another

chemical patterning method, electrochemical DPN,¹⁵⁻²⁰ using a voltage biased AFM tip, can induce electrochemical reactions such as polymerization and oxidation. These processes can take place as an electrochemical bridge¹⁵⁻²⁰ between tip and substrate, which allows one to fabricate nanoscale patterns on electroactive films. For example, cobalt magnetic nanostructures were fabricated by localized electrochemical reduction of Co ions with electrochemical dip-pen lithography (EDPN).²¹ Electrochemical oxidation of poly(vinylcarbazole) (PVK) films on Au substrates has for example been demonstrated.²² The nano electro oxidation, developed by Sagiv and co-workers, electrochemically converts the terminal methyl group of an octadecyltrichlorosilane (OTS) coated silicon layer to a hydrophilic, carboxylic acid-terminated (OTS_{ox}) terminated surface by a voltage-biased conducting AFM tip.²³ Organic thin films such as OTS, PVK, SU-8 epoxy, polythiophene and azobenzene containing ultrathin layers have been used to fabricate nanopatterns by EDPN.²²⁻²⁷

Exploring other suitable polymeric materials with electrochemical patterning capabilities is important for a range of specific applications. Poly(ferrocenylsilanes) (PFS), which contain a main chain with alternating ferrocene and silane units,^{28, 29} can potentially function as a redox responsive platform for EDPN. Water-soluble PFS polyelectrolytes have been assembled with the layer by layer (LbL) technique into multilayer thin films, or microcapsules, and have been described in the literature.³⁰⁻³⁵ In this present communication, we report on the generation of topological and chemical patterns on PFS multilayer thin films by EDPN. Within the scope of this work, rapid direct writing of oxidized PFS polymer at the nanoscale has been demonstrated. The influence of writing parameters such as writing speed, bias voltage, and film thickness were explored and studied to demonstrate line width and pattern geometry control. To the best of our knowledge, this is the first report on local oxidation of organometallic multilayers by directly writing nanopatterns on polymer thin films by EDPN under ambient conditions. This nanopatterning procedure not only has high potential for nanodevice fabrication but also provides a platform to explore the fundamental mechanism of pattern formation.

Layer by layer (LbL) assembly of PFS multilayers was studied and described previously by our group.³⁰⁻³⁴ The molecular structure of PFS polycations and polyanions used in the present work are shown in Scheme 1. The ferrocene units in the polymer main chain can be oxidized to ferrocenium under an applied electrochemical potential.³⁶ The redox properties of PFS based multilayers have been described in a number of articles, and are not detailed here, the reader is kindly referred to the literature.^{30, 32-34} We only mention here that at sufficiently high voltages complete and reversible oxidation of all ferrocenes in the multilayers can be achieved. In the EDPN experiment the electrochemical signal can be confined to the nanometer scale, determined by the AFM tip geometry and dimensions. EDPN makes use of this confined electrochemical action. Scheme 1 represents the idea of the direct electrochemical DPN with PFS multilayers, and the chemical structure of PFS polyelectrolytes used in this study. As shown, in the EDPN technique a voltage bias is applied either on the conductive AFM tip or on the conductive sample substrate, while the tip surface is wetted by an electrolyte “ink”. During the EDPN process, a NaClO_4 electrolyte “ink” was used, which provided a bridge formed between the tip and the substrate. If sufficient voltage bias is applied, a “nanoelectrochemical” cell is achieved. This results in a localized PFS oxidation in the “nanoelectrochemical” cell, over an area determined by the tip-sample contact. The tip-sample separation is adjusted in the AFM contact mode with a tip set-point such that no mechanical deformation of the surface takes place during “writing”.



Scheme 1. Schematic diagram of the direct EDPN

Initially straight line patterns were “drawn” to identify the opportunities and limitations of the electrochemical lithographic patterning on PFS. A tip bias potential was applied on specific scan lines in the AFM contact mode. Patterning was performed using constant force AFM with feedback loop enabled. Subsequently, in tapping mode experiments, by using a tapping mode tip, the previously patterned area was imaged. In Figure 1b, the morphology of patterned lines is shown. The bias voltage (-7V) results in significant local expansion (elevation) of the PFS multilayer compared to the unpatterned area. Writing without potential on the same substrate did not produce any observable patterns confirming that the lines are not generated via scratching the polymer film surface with the tip. The same experimental procedure was applied to the ITO substrate without polymer films. No obvious pattern was observed on pure ITO (Figure 1a)

either. In a subsequent step, the lithographic ability of the AFM for programmed scan lines was used to write more complex patterns. Short texts such as “MTP” (abbreviating the name of our group, ☺), with a width of 216 nm, were drawn using a tip bias of -7 V (shown in Figure 1c).

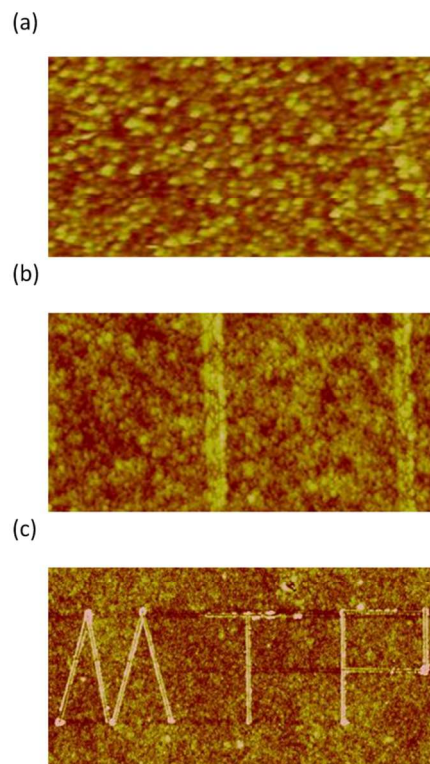


Figure 1. Topography of (a) ITO substrate (scan size $10\mu\text{m}\times 5\mu\text{m}$, Z range is 20 nm); (b) PFS₅ bilayers (scan size $3\mu\text{m}\times 1.5\mu\text{m}$, Z range is 20 nm) showing two EDPN-fabricated lines; (c) PFS₅ bilayers (scan size $10\mu\text{m}\times 5\mu\text{m}$, Z range is 20 nm) with the letters MTP. (Patterning conditions: tip bias voltage -7V at a scan speed of $2\mu\text{m/s}$ under 30% of humidity).

Subsequently, the bias voltage dependence of the nanopatterns was examined. Bias potentials of -3, -4, -5, -6, and -7V were applied on the tip for pattern drawing. The morphology of the nanolines obtained with different tip bias potential is shown in Figure 2a. The cross section of the nanolines and dimension (height and width) of the lines are illustrated in Figure 2b and 2c, respectively. A variation of pattern width and height with respect to the applied bias was observed. The oxidized polymer lines are characterized by a height and width increase over the applied potential owing to the electrochemical oxidation process. Higher voltages afford thicker and broader structures than lower ones. The dependence of feature aspect ratio values on the bias voltage of the patterns shown in Figure 2 varies from 11.6 (at -4 V), 13.6 (at -5V), 13.4 (at -6V) to 12.4 (at -7 V). The pattern size dependence on the bias is a clear indication that the electric field plays an important role in the process. With EDPN, no obvious pattern was observed by setting the bias to -3V, while the electrolyte bridge was maintained. The ability to turn off the writing with potential control also allows repeated patterning with

the electrolyte ink-coated tip at very slow speeds for many hours, which is a feature not possible with DPN.

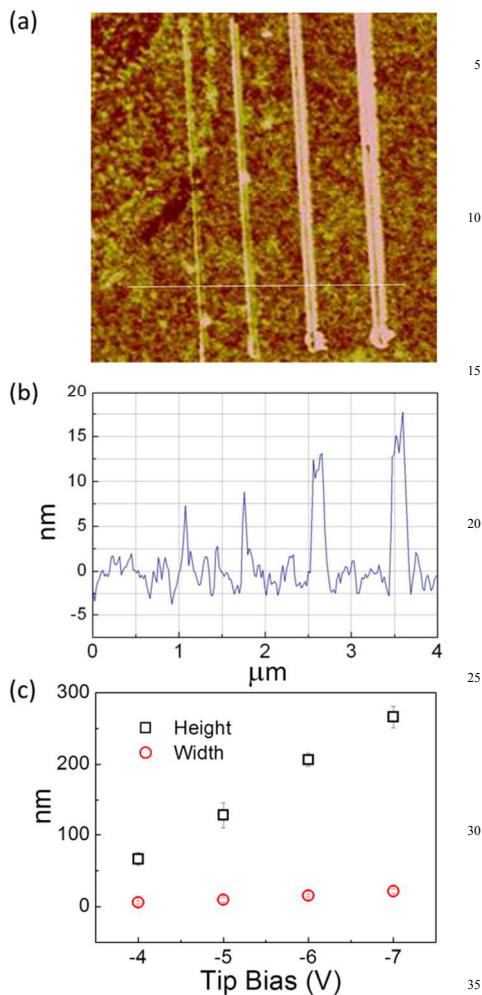


Figure 2. (a) Topography of PFS₅ bilayers as shown by tapping mode height images (scan size 5 μm × 5 μm, Z range is 10 nm), capturing electrochemically oxidized nanolines (patterning condition: tip bias voltage of -4, -5, -6, and -7V from left to right, at a scan speed of 2 μm/s under 30% of humidity); (b) cross section of nanolines obtained along the section shown in Figure 2a; (c) the height and width of nanolines formed under different bias potentials.

We described earlier the relationship between PFS multilayer thickness and the number of deposited bilayers, as a function of electrolyte concentration, in a separate study.³²⁻³⁴ Based on this knowledge, we varied the LbL film thickness to study its influence on the characteristics of the patterns. Figure 3a and 3b show the morphology of nanolines on PFS₅ bilayers and PFS₁₀ bilayers, respectively. We observed that with increasing bilayer number, the width and height of nanolines increased. This is attributed to the increased redox responsive polymer mass in the nanoelectrochemical cell formed.

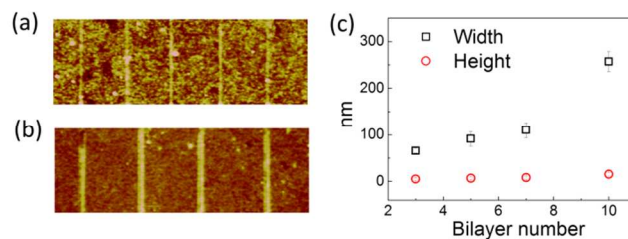
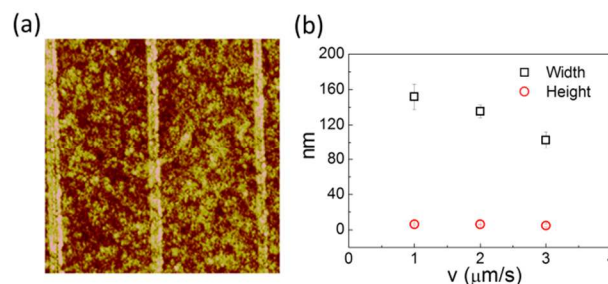


Figure 3. Topography of (a) PFS₅ bilayers (scan size 10 μm × 3.3 μm, Z range is 20 nm) and (b) PFS₁₀ bilayers (scan size 10 μm × 3.3 μm, Z range is 20 nm) displaying electrochemically oxidized nanolines (patterning condition: tip bias voltage -7V, at a scan speed of 2 μm/s under 30% of humidity); (c) the height and width values formed on films with different bilayer number as a function of the bilayer number.

Figure 4 shows three lines fabricated at different scanning speeds illustrating that the dimensions of the structures obtained also depend on the scanning speed. Slower speeds yield wider features than those fabricated at higher speeds. However we note that the height of the nanolines shows only a small variation.

In order to interpret the above observations, we tentatively propose the following mechanism for the line formation. During electrochemical oxidation in the nanoelectrochemical cell PFS is converted to PFS_{ox} through electrochemical oxidation that occurs between the tip and PFS thin film. Local oxidation depends on the presence of the electrolyte, and its permeation into the multilayer. This is scan rate dependent, which determines the line



with resolution via “electrolyte ink diffusion” causing broadening for slower scan rates.

Figure 4. Topography of a PFS₅ bilayers film (scan size 5 μm × 5 μm, Z range is 10 nm) featuring electrochemically oxidized nanolines (patterning condition: tip bias voltage of -7V at a scan speed of 1, 2 and 3 μm/s under 30% of humidity); (b) the height and width of nanolines formed with different writing speed.

During the electrochemical writing, ferrocenium cations form, whose charge is compensated by ions transferred in the nanoelectrochemical cell. This process adds mass to the oxidized areas, thus contributes to the elevation of the oxidized lines. However, other factors must also be considered. On the basis of previous work reported by Lyuksyutov et al.¹⁰, it can be hypothesized that the attractive electrostatic force between the charged tip and the electron rich film is strong enough to draw the softened polymer toward the tip, if the film is deformable (by

plastic or viscoelastic deformation, for example). Current flow through a thin polymer film, arising from a bias between a conductive substrate and AFM tip, results in localized Joule heating of the polymer and increases the temperature to above its T_g (29.5°C).³⁷ The extremely non uniform electric field gradients near the tip may polarize the softened polymers and lift patterns by mass transfer.¹⁰ To address the effect of possible Joule heating, a square shaped section of a multilayer film was patterned by tapping mode, by scanning across a 2.5 $\mu\text{m} \times 2.5 \mu\text{m}$ area with a scan speed of 1.5 Hz at +5 V sample bias. Figure 5a shows the square pattern obtained, which exhibits an average elevation of 4 nm. The corresponding phase image (Figure 5b) shows that the patterned area has different phase contrast, which is rationalized by the deposition of the perchlorate anions from the electrolyte. We note finally that at this point we are unable to separate the contributions that arise from PFS oxidation and perchlorate deposition from Joule heating effects.

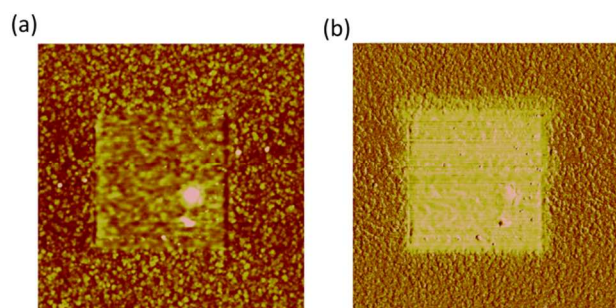


Figure 5. Tapping mode EDPN on a PFS₅ multilayer (scan size 5 $\mu\text{m} \times 5 \mu\text{m}$); (a) height image (Z range is 40 nm); (b) phase image (Z range is 10 °) of an electrochemically oxidized square shaped domain (patterning condition: sample bias voltage of +5V at a speed of 2 $\mu\text{m}/\text{s}$ under 80% of humidity).

Finally we note that in order to assess the electrical properties of the PFS multilayers, I/V curves were measured with conducting AFM. The band gap value of the PFS₅ bilayer obtained from these I/V curves was 4.9 eV. The details of the experiment were presented in EIS. This experiment confirms the semiconducting character of PFS, which is relevant for electron transfer during patterning.

Conclusions

AFM assisted electrochemical DPN was performed on PFS multilayers to create surface patterns formed due to alteration of surface composition (anion deposition from bridging electrolyte “ink”), polymer oxidation state, and topography in the patterned areas. The width and height of line patterns increase linearly with bias voltage, multilayer number and decrease with writing speed. The pattern formation was attributed to local oxidation of PFS, with deposited anions from the electrolyte to ensure charge neutrality, in possible combination with Joule heating effects. This study demonstrates that PFS multilayers form promising substrates for facile surface nanopatterning to be potentially used in various nanotechnology applications.

Acknowledgements

We are grateful to A*STAR (Agency for Science, Technology and Research) Institute of Materials Research and Engineering (IMRE) Singapore and to the MESA⁺ Institute for Nanotechnology of the University of Twente for providing financial support.

Notes and references

^a Institute of Materials Research and Engineering, A*STAR (Agency for Science, Technology and Research), Research Link 3, 117602, Singapore. Tel: (65) 6874 7903; Fax: (65) 6872 0875; E-mail: songji@imre-a-star.edu.sg

^b MESA⁺ Institute for Nanotechnology, Materials Science and Technology of Polymers, University of Twente, P.O. Box 217, 7500 AE Enschede, the Netherlands. Tel: (31) 53 489 2974; Fax: (31) 53 489 3823; E-mail: g.j.vancso@utwente.nl

^c Data Storage Institute, A*STAR (Agency for Science, Technology and Research), 5 Engineering Drive 1, 117608, Singapore. Tel: (65) 6874 8630; Fax: (65) 6776 6527; E-mail: CHUNG_Hong_Jing@dsi-a-star.edu.sg

†Electronic Supplementary Information (ESI) available. See DOI: 10.1039/b000000x/

- B. Adhikari and S. Majumdar, *Prog. Polym. Sci.*, 2004, **29**, 699-766.
- Q.-D. Ling, D.-J. Liaw, E. Y.-H. Teo, C. Zhu, D. S.-H. Chan, E.-T. Kang and K.-G. Neoh, *Polymer*, 2007, **48**, 5182-5201.
- B. W. Maynor, S. F. Filocamo, M. W. Grinstaff and J. Liu, *J. Am. Chem. Soc.*, 2002, **124**, 522-523.
- D. S. Ginger, H. Zhang and C. A. Mirkin, *Angew. Chem., Int. Ed.*, 2004, **43**, 30-45.
- N. L. Rosi and C. A. Mirkin, *Chem. Rev.*, 2005, **105**, 1547-1562.
- G. Agarwal, R. R. Naik and M. O. Stone, *J. Am. Chem. Soc.*, 2003, **125**, 7408-7412.
- J. H. Lim and C. A. Mirkin, *Adv. Mater.*, 2002, **14**, 1474-1477.
- R. D. Piner, J. Zhu, F. Xu, S. H. Hong and C. A. Mirkin, *Science*, 1999, **283**, 661-663.
- J. Q. Song, Z. F. Liu, C. Z. Li, H. F. Chen and H. X. He, *Appl. Phys. A-Mater.*, 1998, **66**, S715-S717.
- S. F. Lyuksyutov, R. A. Vaia, P. B. Paramonov, S. Juhl, L. Waterhouse, R. M. Ralich, G. Sigalov and E. Sancaktar, *Nat. Mater.*, 2003, **2**, 468-472.
- J. Duvinneau, H. Schonherr and G. J. Vancso, *ACS Nano*, 2010, **4**, 6932-6940.
- A. W. Knoll, D. Pires, O. Coulembier, P. Dubois, J. L. Hedrick, J. Frommer and U. Duerig, *Adv. Mater.*, 2010, **22**, 3361-3365.
- S. Kinge, M. Crego-Calama and D. N. Reinhoudt, *Chemphyschem*, 2008, **9**, 20-42.
- K. H. A. Lau, J. Bang, D. H. Kim and W. Knoll, *Adv. Func. Mater.*, 2008, **18**, 3148-3157.
- Q. Hao, X. Xie, W. Lei, M. Xia, F. Wang and X. Wang, *J. Phys. Chem. C*, 2010, **114**, 9608-9617.
- C. Huang, G. Jiang and R. Advincula, *Macromolecules*, 2008, **41**, 4661-4670.
- B. W. Maynor, J. Y. Li, C. G. Lu and J. Liu, *J. Am. Chem. Soc.*, 2004, **126**, 6409-6413.
- H.-J. Son, W.-S. Han, S. J. Han, C. Lee and S. O. Kang, *J. Phys. Chem. C*, 2010, **114**, 1064-1072.
- L. Zeng, Z. Le, J. Xu, H. Liu, F. Zhao and S. Pu, *J. Mater. Sci.*, 2008, **43**, 1135-1143.
- Y. Zhang, K. Salaita, J. H. Lim and C. A. Mirkin, *Nano Lett.*, 2002, **2**, 1389-1392.
- H. Chu, S. Yun and H. Lee, *J. Nano Sci. Nano Technol.*, 2013, **13**, 8055-8058.

22. S. Jegadesan, P. Taranekar, S. Sindhu, R. C. Advincula and S. Valiyaveetil, *Langmuir*, 2006, **22**, 3807-3811.
23. A. Zeira, J. Berson, I. Feldman, R. Maoz and J. Sagiv, *Langmuir*, 2011, **27**, 8562-8575.
- 5 24. A. Baba, G. Jiang, K.-M. Park, J.-Y. Park, H.-K. Shin and R. Advincula, *J. Phys. Chem. B*, 2006, **110**, 17309-17314.
25. Y. G. Cai and B. M. Ocko, *J. Am. Chem. Soc.*, 2005, **127**, 16287-16291.
26. G. Jiang, A. Baba and R. Advincula, *Langmuir*, 2007, **23**, 817-825.
- 10 27. C. Martin-Olmos, L. G. Villanueva, P. D. van der Wal, A. Llobera, N. F. de Rooij, J. Brugger and F. Perez-Murano, *Adv. Func. Mater.*, 2012, **22**, 1482-1488.
28. V. Bellas and M. Rehahn, *Angew. Chem., Int. Ed.*, 2007, **46**, 5082-5104.
- 15 29. J.-C. Eloi, D. A. Rider, G. Cambridge, G. R. Whittell, M. A. Winnik and I. Manners, *J. Am. Chem. Soc.*, 2011, **133**, 8903-8913.
30. Y. Ma, W.-F. Dong, M. A. Hempenius, H. Mohwald and G. J. Vancso, *Nat. Mater.*, 2006, **5**, 724-729.
- 20 31. Y. Ma, W.-F. Dong, E. S. Kooij, M. A. Hempenius, H. Moehwald and G. J. Vancso, *Soft Matter*, 2007, **3**, 889-895.
32. J. Song, D. Janczewski, Y. Ma, M. Hempenius, J. Xu and G. J. Vancso, *J. Colloid Interf. Sci.*, 2013, **405**, 256-261.
- 25 33. J. Song, D. Janczewski, Y. Ma, M. Hempenius, J. Xu and G. J. Vancso, *J. Mater. Chem. B*, 2013, **1**, 828-834.
34. J. Song, D. Janczewski, Y. Ma, L. van Ingen, C. E. Sim, Q. Goh, J. Xu and G. J. Vancso, *Eur. Polym. J.*, 2013, **49**, 2477-2484.
- 30 35. Z. Y. Zhong, C. Lin, Y. Ma, M. A. Hempenius, M. C. Lok, M. M. Fretz, J. F. J. Engbersen, G. J. Vancso, W. E. Hennink and J. Feijen, *J. Control. Release*, 2006, **116**, E81-E83.
36. R. Rulkens, A. J. Lough, I. Manners, S. R. Lovelace, C. Grant and W. E. Geiger, *J. Am. Chem. Soc.*, 1996, **118**, 12683-12695.
- 35 37. R. G. H. Lammertink, M. A. Hempenius, I. Manners and G. J. Vancso, *Macromolecules*, 1998, **31**, 795-800.